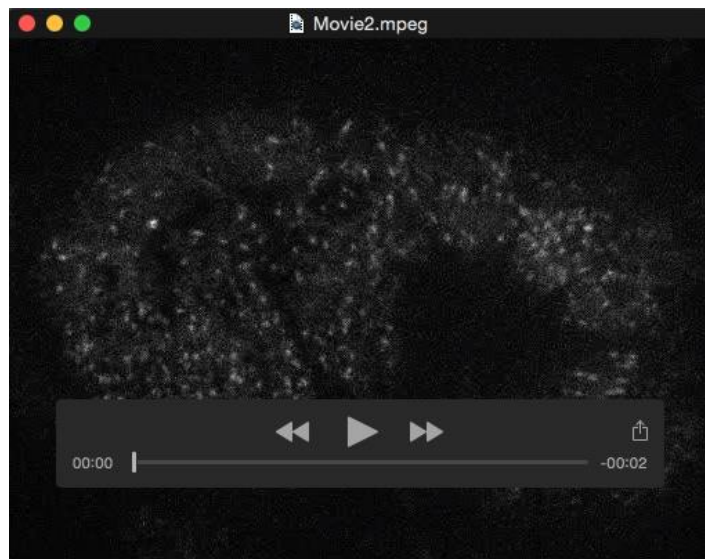


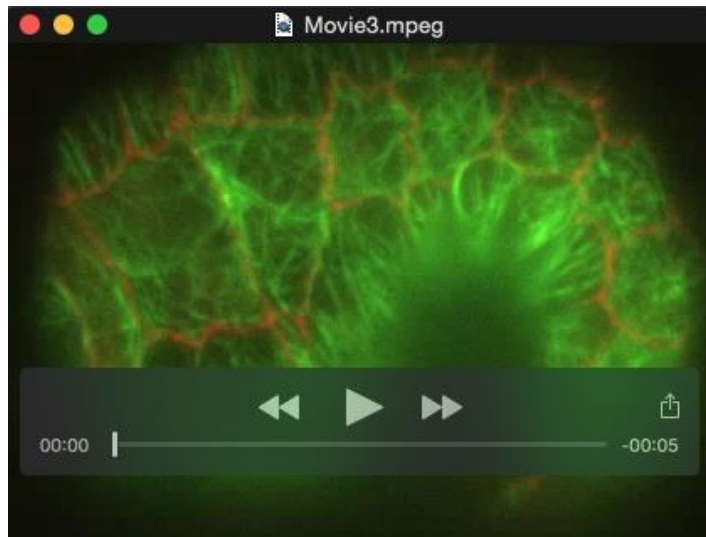
Movie 1. Microtubule dynamics in the epidermis of *C. elegans* elongating embryo.

Five-dimensional time-lapse (xyztλ) of a wild-type embryo expressing EBP-2::GFP and DLG-1::RFP. Images are maximum intensity projections of 4 z planes acquired in the GFP and RFP channels, separated by 0.3 μm steps. 40 stacks were acquired every 500ms during 32 sec (total movie time). Movie is played back in 32X real time. This movie illustrates how microtubules come in close contact with adherens junctions and the difference in microtubule behavior between seam cells and ventral cells. For EB1 quantifications, the GFP channel was acquired alone (see Movie 2); a single RFP image was generated at the end of the movie in order to visualize cell borders.



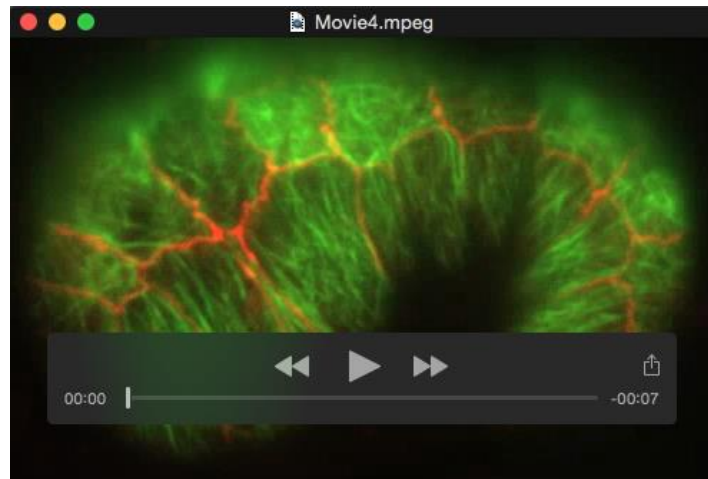
Movie 2. Typical EB1 movie used for quantifications.

Four-dimensional time-lapse (xyzt) of a wild-type embryo expressing EBP-2::GFP. Images are maximum intensity projections of 3 z planes (0.3 μ m step). 100 stacks were acquired as fast as possible during 30 sec. Movie is played back in 10X real time.



Movie 3. Microtubules dynamics in epidermal seam cells.

Time-lapse movie of a control embryo expressing DLG-1::RFP and TBA-2::GFP, labeling junctions and microtubules, respectively. Images were acquired every 200 ms, time-averaged over 10 frames, and played back in 30X real time. The red channel has been acquired before the imaging starts to position the junctions. This movie illustrates that microtubules polymerize in dorsal ventral towards seam-dorso-ventral junctions. In addition, microtubules originate from aster-like structures (potentially corresponding to bundled microtubules) in the seam cells, or occasionally from seam junctions (especially in the body).



Movie 4. Microtubules dynamics in epidermal ventral cells.

Time-lapse movie acquired in the same conditions as Movie 3. This movie shows that microtubules polymerize from the region corresponding to hemidesmosomes.



Movie 5. E-cadherin mobile fraction is lower in *let-502; spas* *OE* embryos.

Fluorescence recovery after photobleaching (FRAP) movie of a control (left) and a *let-502; spas* *OE* mutant (right) expressing the E-cadherin HMR-1::GFP reporter. Images are 152 single z planes acquired during 3:min 55s. The arrow indicates the photobleached junction. Movie is played back in 47X real time.



Movie 6. Intracellular E-cadherin vesicles movements are limited in *let-502; spas* *OE* embryos.

Movie of a control (left) and a *let-502; spas* *OE* mutant (right) expressing the E-cadherin HMR-1::GFP reporter. E-cadherin-positive vesicle movements are obvious in the control while their amplitude is more limited in the double mutant. Images are 120 single z planes acquired at 2 images/sec. This movie has been corrected for photobleaching by the histogram matching method, and is played back in 10X real time.

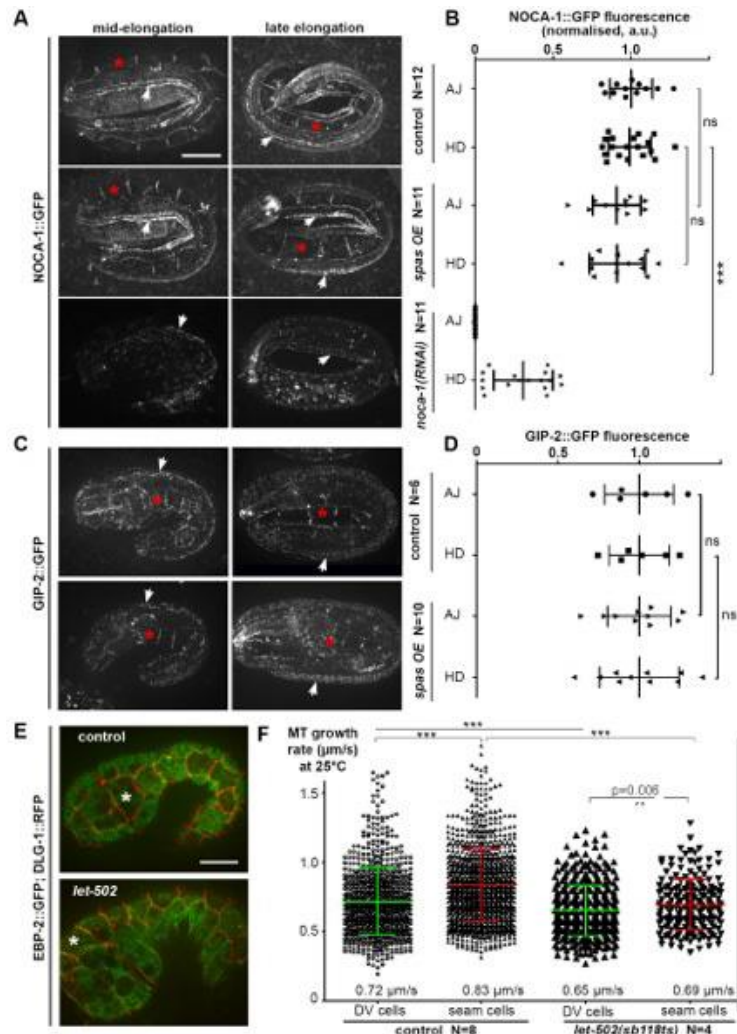


Fig. S1. NOCA-1 and GIP-2 reporter localizations are microtubule-independent.

Confocal spinning-disc images of embryos expressing the NOCA-1::GFP (A) and GIP-2::GFP (C) reporters in the indicated backgrounds (right), at two different stages. (B, D) Quantification of the fluorescence intensity of adherens junctions (AJ) between seam cells (asterisk) and hemidesmosomes (HD, arrowhead) in these embryos, showing that *spas* *OE* embryos express the two reporters at levels comparable to that of controls, whereas *noca-1*(*RNAi*) embryos show a markedly reduced intensity of NOCA-1::GFP. Fluorescence intensities were normalized to control average intensity. Bars indicate mean and s.d., ns non significant, *** p<0.001 (E-F) Microtubule growth rates in wild-type and *let-502* embryos. (E) Spinning-disc confocal 4D projections from movies of embryos co-expressing the EBP-2::GFP and the junction DLG-1::RFP reporters (to visualize cell borders), grown at 25°C. (F) Scatter dot plot of the microtubule (MT) growth rate ($\mu\text{m/s}$) extracted from the movies, in dorso-ventral (DV) and in seam cells. In *let-502*(*sb118ts*) mutants, microtubules polymerize slower, and the growth rate difference between seam and DV cells is attenuated. Control: N=803 tracks in DV cells, N=1045 in seam cells, in 8 embryos analyzed. *let-502*(*sb118ts*): N=416 tracks in DV cells, N=198 in seam cells, in 4 embryos analyzed. Bars indicate mean and s.d., *** p<0.001

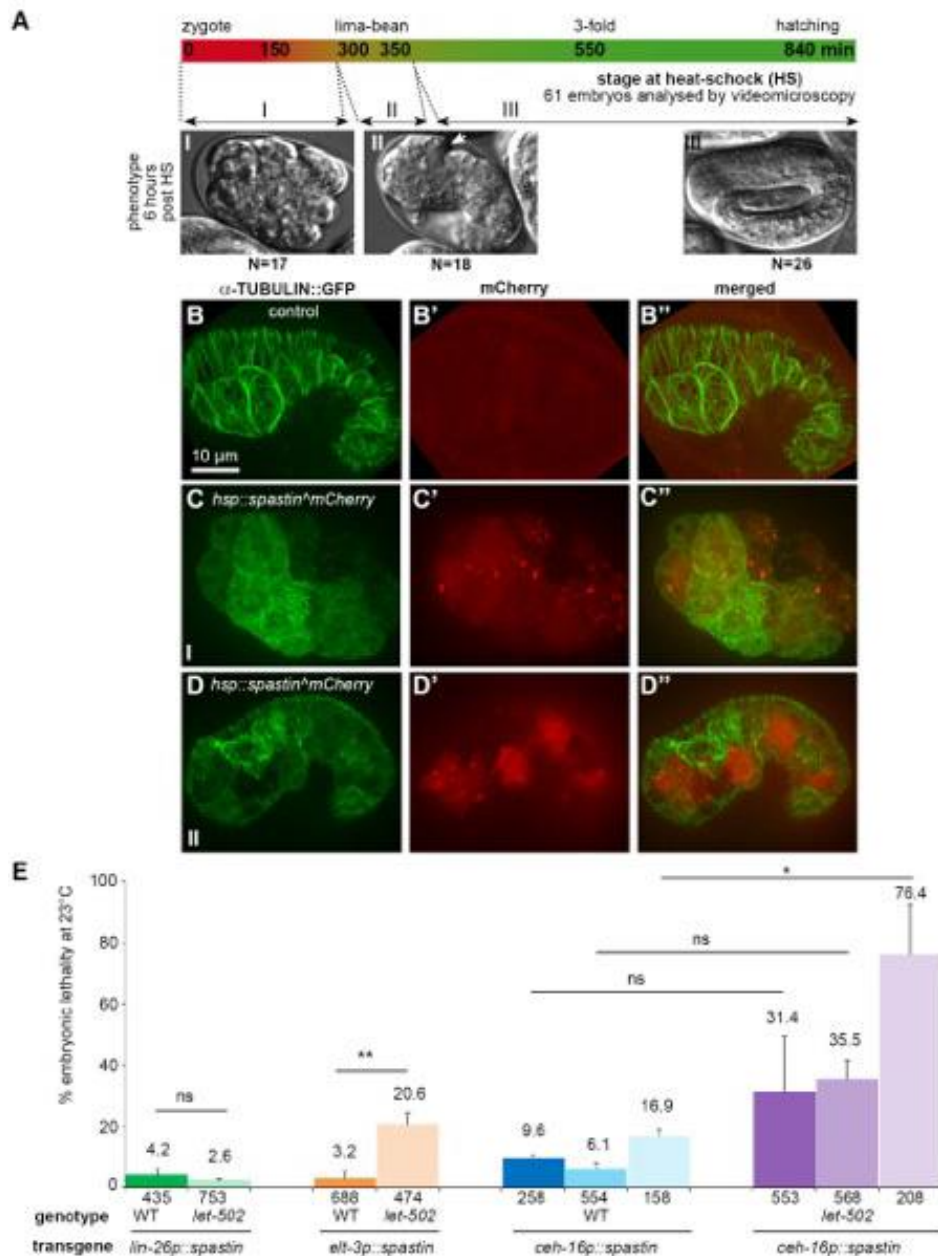


Fig. S2. Heat-shock Spastin efficiently degrades microtubules in early embryos and epidermal Spastin triggers low lethality.

(A) Color bar representing the time scale of embryonic development, and the different time windows (double-side arrows 1, 2 and 3) at which the 61 *hsp::spastin* transgenic embryos were subjected to a heat-shock (HS) treatment. (B) DIC images corresponding to the stage reached 6 hours post-HS for the 3 classes of embryos. In class I embryos (early HS), blastomeres stopped dividing, resulting in a premature developmental arrest (N=17). Class II embryos (HS around the lima-bean stage) arrested during elongation (N=18) and often show bulges (arrowhead). These embryos have large cells, their number has not been precisely counted. Class III embryos (HS after the comma stage) continued to develop normally (N=26). (B-D'') Confocal spinning-disc projections of

embryos expressing the α -tubulin reporter (B-B'', control) and the *hsp::spastin* construct (C-D series, class I and II respectively). For each genotype, the corresponding mCherry channel (B'C'D') and the resulting merged image (B''C''D'') are shown. Note the strong microtubule degradation in all mCherry-positive cells. (E) Bar graph showing the embryonic lethality in various transgenic lines expressing Spastin under different epidermal promoters (*lin-26p*, pan-epidermal; *elt-3p*, dorso-ventral cells, *ceh-16p*, seam cells, for which three independent lines are shown). Bars indicate mean and s.d., ns non significant, * p<0.05 *** p<0.001.

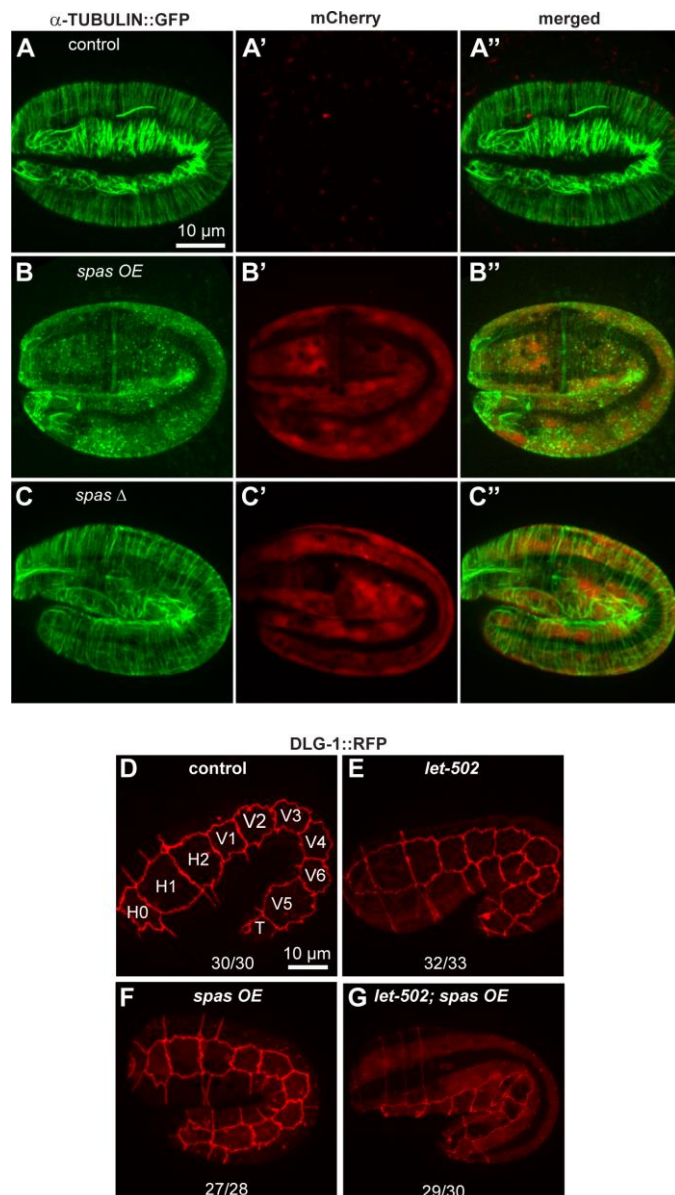


Fig. S3. Epidermal Spastin expression triggers microtubules degradation without affecting epidermal cells number or the DLG-1 reporter.

(A-D) Confocal spinning-disc projections of embryos expressing the junction reporter DLG-1::RFP; the 10 seam cells are named in the control (H0-H2, V1-V6, T). For each genotype, the bottom numbers indicate in how many embryos the correct number of seam cells has been counted. Note that epidermal Spastin expression did not affect seam cells division, and that the DLG-1::RFP pattern is unaffected in *spas OE* embryos. (E-G") Confocal spinning-disc projections of embryos expressing the α -tubulin reporter (E-E", control) and the *dpy-7p::spastin* construct (F-F") or a deleted control version *dpy-7p::spastin Δ* (G-G"; see Fig. 3A the position of the deletion). For each embryo, the corresponding mCherry channel (E'F'G') and the merged image (E" F" G") are shown. In F, microtubules have a degraded dotty appearance (quantified in Fig. 3C), whereas in G they still appear linear, indicating that only full-length Spastin could trigger a deleterious effect.

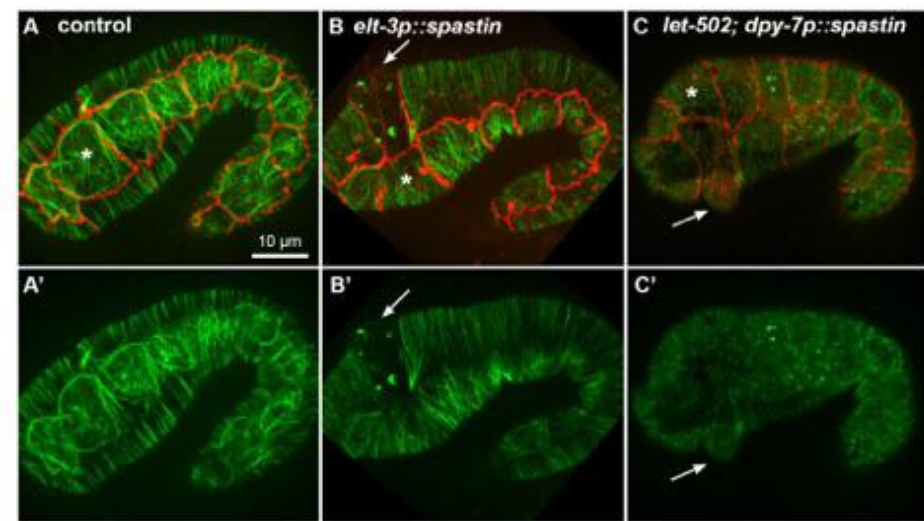


Fig. S4. Spastin expression induces bulges, especially in the head.

(A-C) Confocal spinning-disc projections of embryos co-expressing the α -tubulin and the junction DLG-1::RFP reporters, in wild-type (A), *elt-3p::spastin* (B), and *let-502(sb118ts); dpy-7p::spastin* (C) backgrounds. (A'-C') Same embryos as on top but only the green channel (TBA-2::GFP) is shown. In B, mosaic embryo where only two dorsal cells express a high level of Spastin and form a protrusion (arrow). A protuberance is also apparent in a ventral cell of the head in C (arrow; observed in 17/24 *let-502; spas* OE embryos). Asterisks, seam cells position.

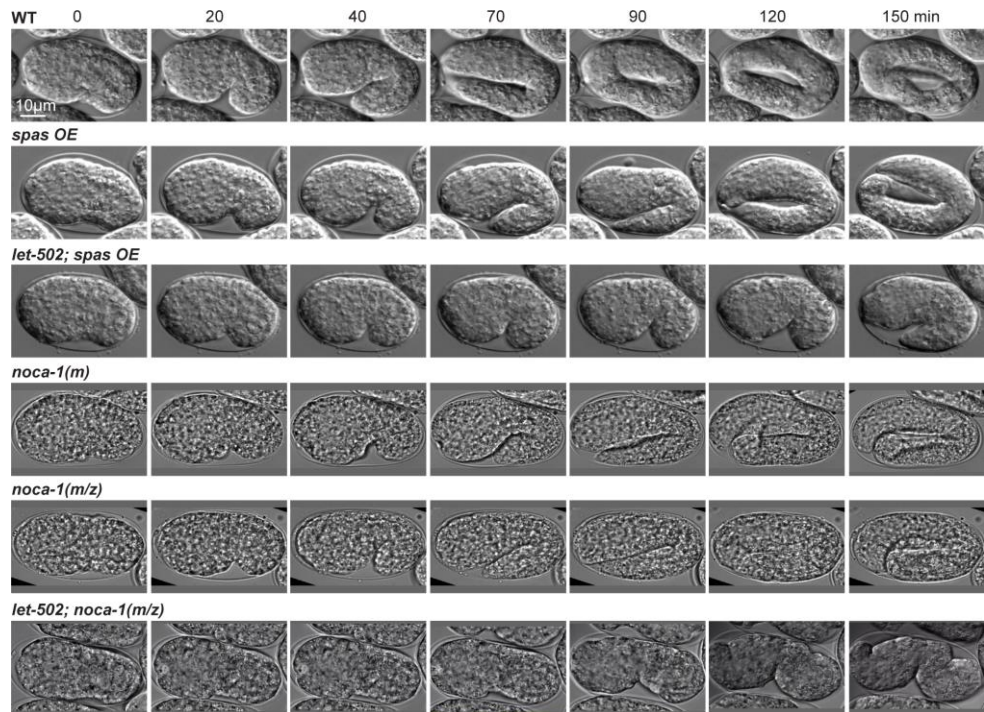


Fig. S5. Stills extracted from timelapse DIC movies.

DIC images were extracted from videomicroscopy analyses on embryos, allowed to develop on a microscope stage set on 23°C. Time (min) is indicated. *spas* *OE* embryos, *noca-1(m)* and *noca-1(m/z)* mutant develop slower than controls but reach the final stage of elongation. By contrast, both *let-502; spas* *OE* and *let-502, noca-1(m/z)* have a very slow pace of development (quantified in Fig. 4C) and eventually fail to elongate. This presentation was preferred to movies, to allow a better comparison between genotypes.

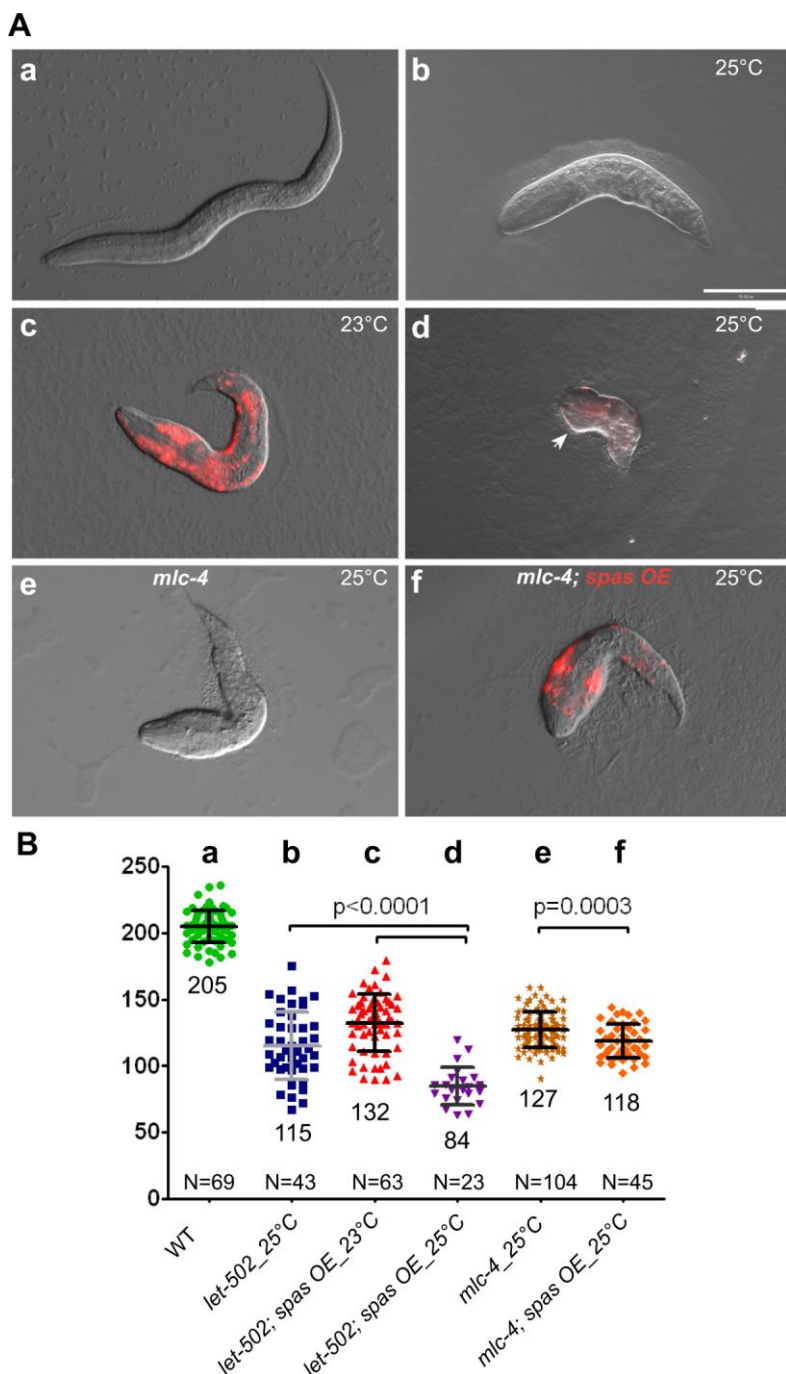


Fig. S6. Spastin expression has more dramatic effects in *let-502* than in *mlc-4* mutant backgrounds.

(A) DIC images of representative hatchlings. In c, d and f, the mCherry channel has been superposed to visualize Spastin expression. Note the bulge in the head of the *let-502; spas OE* larva (d, arrowhead). (B) Scatter dot plots showing the body length (μm) of newly hatched larvae shown in A. Identical lower case letters in A and B correspond to the same genotypes (indicated). Note the amplitude of size difference between b-d (major reduction of size in *let-502; spas OE*) and e-f (minor reduction in *mlc-4; spas OE*). Bars indicate mean and s.d.

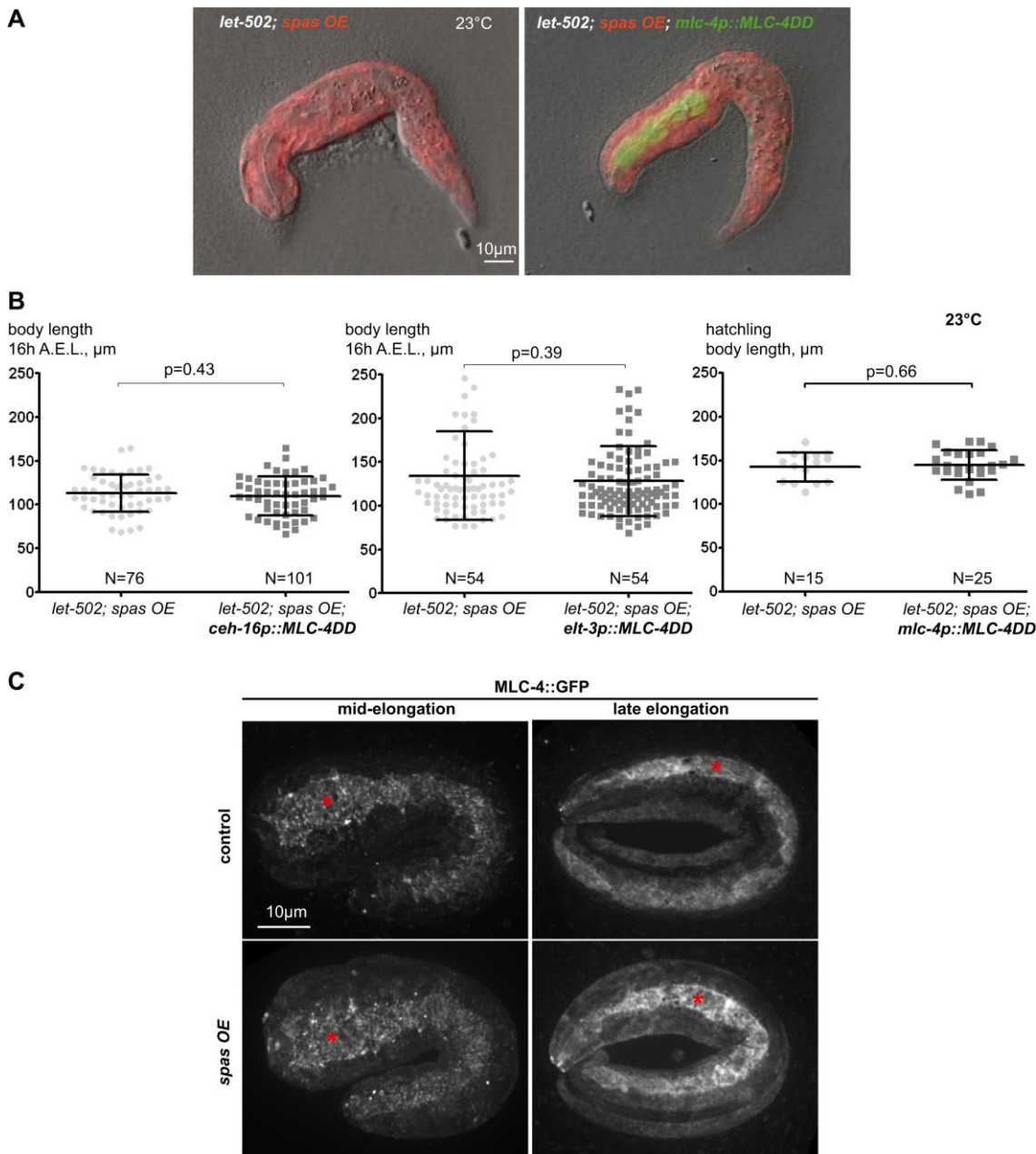
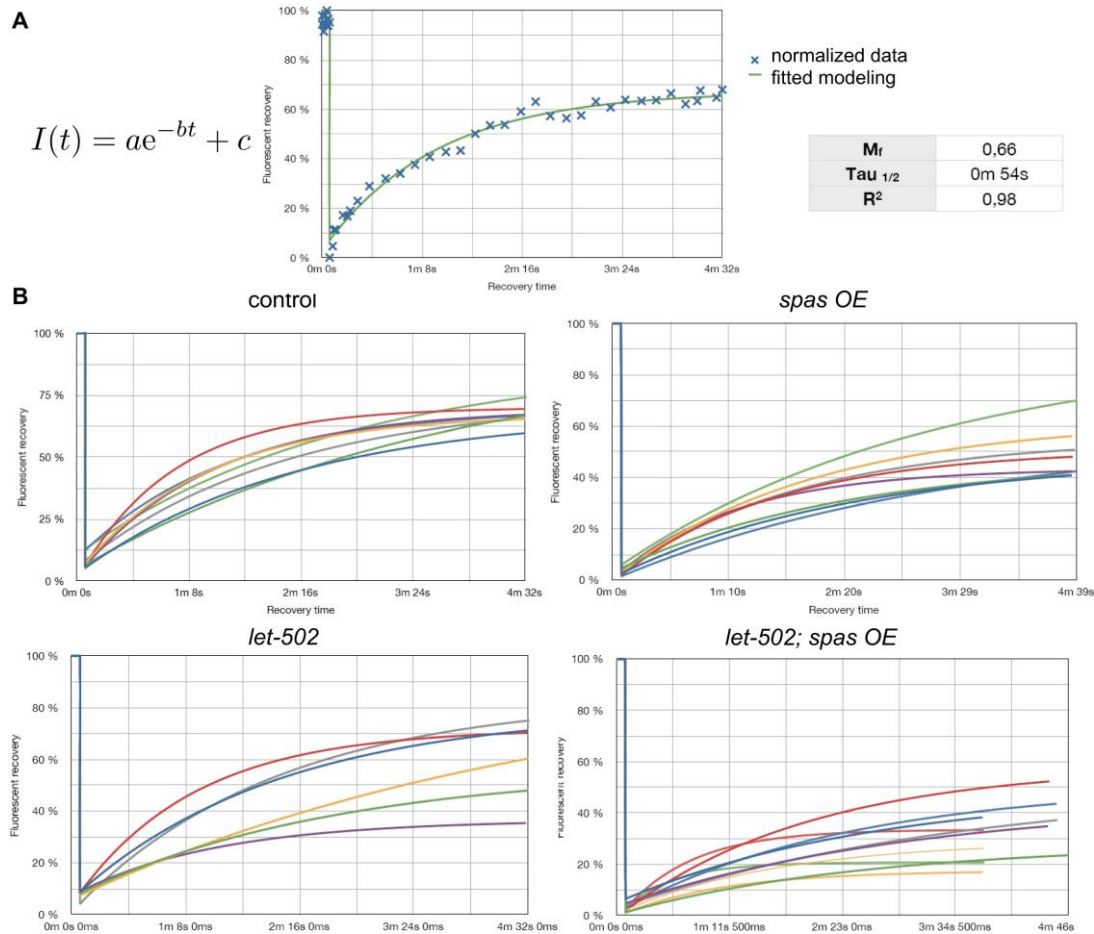


Fig. S7. Restoring myosin II activity in *let-502; spas OE* animals does not rescue the elongation defect.

(A) DIC images of representative *let-502; spas OE* larvae. Both the mCherry and the GFP channels were superposed to visualize the presence of the MLC-4DD transgene —in which the regulatory Myosin Light Chain residues Ser18 and Thr19 phosphorylated by ROCK have been mutated to Asp— attested by the presence of the pharyngeal MYO-2::GFP co-injection marker. Note that the two larvae appear very similar in size. (B) Scatter dot plots showing the body length (μm) of *let-502; spastin* larvae expressing (or not) the constitutively active form of myosin II (MLC-4-DD) under different promoters: *mlc-4p* for the endogenous pattern, *ceh-16p* for lateral cells, and *elt-3p* for dorso-ventral cells. All measurements were done at 23°C A.E.L., after egg laying. None of the constructs

significantly rescued the elongation, as attested by the p value. Bars indicate mean and s.d. (C) MLC-4::GFP is not affected upon Spastin expression. Confocal spinning-disc top projections of embryos expressing the myosin II regulatory subunit reporter MLC-4::GFP construct, at two different stages. *spas OE* embryos (bottom) show a similar pattern compared to the control (top), with an enrichment of MLC-4::GFP in the seam cells (asterisk).

**Fig. S8. Individual FRAP curves.**

(A)- Exponential formula used to fit a curve on the FRAP experimental data (see Methods). The graph shows an illustration for a control embryo. Mobile fraction, half-time recovery (tau) and coefficient of determination (R^2 , goodness of fit), are indicated in this example. (B)- Individual fitted curves for all analyzed genotypes, corresponding to the average bar graph shown in Fig. 5K.

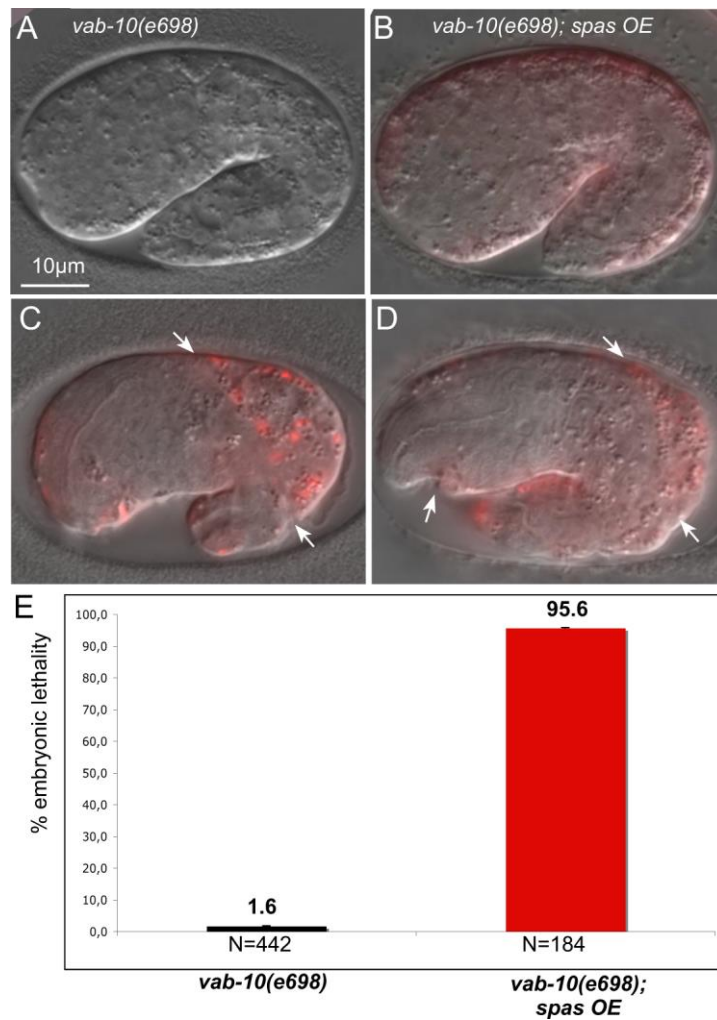


Fig. S9. Spastin expression and weakened hemidesmosomes prevent embryonic elongation.

(A-D)- DIC images of *vab-10(e698)* embryos (A) and *vab-10(e698); spas OE* mutants (B-D), in which the mCherry channel has been superposed. Initially, double mutants are normal (B), but they stop elongating when muscles become active, showing signs of muscles detachments (23/28 embryos, arrows, C-D). (E) Bar graph displaying the percentage of embryonic lethality in these strains.

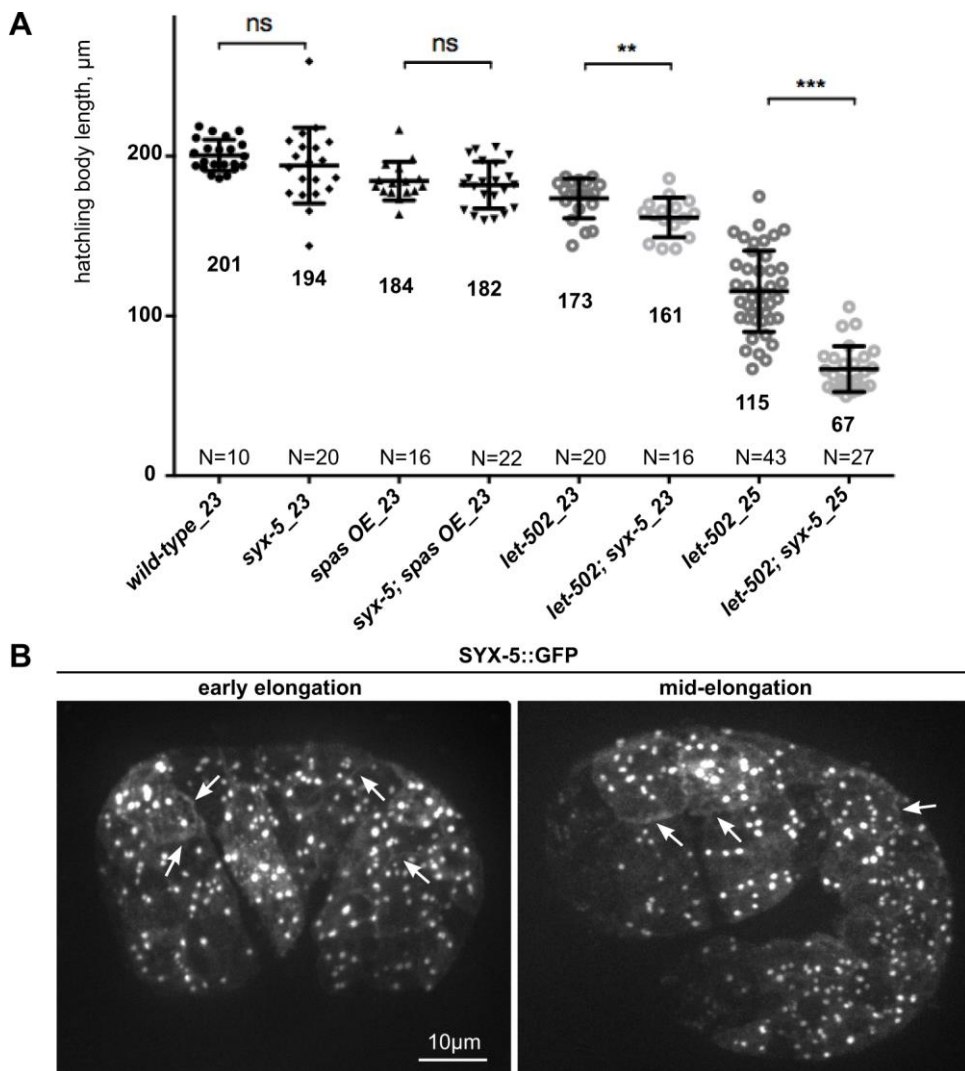


Fig. S10. SYX-5::GFP localizes as puncta and along adherens junctions in the epidermis.

(A)- Body size measurements of newly hatched larvae of the indicated genotypes at the indicated temperatures (below). Note that *syx-5* loss of function enhances the phenotype of *let-502* animals but does not affect that of *spas OE* animals.

(B)- Confocal spinning-disc projections of embryos expressing the SYX-5::GFP construct at two different stages. The predominant pattern is punctate (presumably corresponding to the Golgi apparatus), and a faint GFP signal is detected at the level of junctions (arrows). Bars indicate mean and s.d., ns non significant, ** p<0.01 *** p<0.001.

Table S1. Raw data of the enhancer screen for *let-502* at 23°C.

The 237 genes were selected on Wormbase, mostly for microtubule-related and transport-related processes. In addition, some genes were used as controls (asterisks, include some house-keeping genes), for which the RNAi depletion was supposed to induce a strong phenotype. Emb, early Embryonic lethality, Bmd, Body Morphological Defects. Screen hits were considered as positive when Bmd % reached at least 30%. The hits presented in Fig. 7 and Table 1 were further validated.

Gene name	Known ortholog	RNAi phenotype in wild-type	RNAi phenotype <i>let-502</i> (<i>sb118ts</i>) at 23°C
L4440 empty vector *		WT	WT
<i>dhc-1</i> / T21E12.4	Dynein heavy chain	WT	5% Emb; 5% Bmd
<i>klp-15</i> / M01E11.6	Kinesin family member 15	30% Emb	40% Emb; 10% Bmd
<i>kca-1</i> / C10H11.10	Kinesin cargo adaptor	WT	10% Bmd
<i>pfd-6</i> / T21E12.4	Prefoldin 6 subunit	WT	10% Bmd
<i>mei-2</i> / F57B10.12	p80 subunit of katanin	60-70% Emb	70-80% Emb
<i>che-3</i> / F18C12.1	dynein heavy chain 1b isoform	WT	WT
<i>mei-1</i> / T01G9.5	catalytic subunit of katanin	30-40% Emb	60% Emb
<i>klp-16</i> / C41G7.2	Motor kinesin Kar3/Ncd	30% Emb	10% Emb
<i>dlc-6</i> / Y106G6G.3	Dynein light chain/ DYNLL1&2	WT	10%Emb
<i>pfd-3</i> / T06G6.9	Prefoldin / VBP1	40% Emb	20% Emb + 40% Bmd
F32A7.5	MAP 1	WT	WT
<i>pes-7</i> / F09C3.1	IQGAP	WT	WT
<i>rsa-1</i> / C25A1.9	PP2A regulatory subunit B'' class	5% Emb	5% Emb + 40% Bmd
<i>vab-10</i> / ZK1151.1 *	Spectraplakin / BPAG1	100% Bmd+dead mothers	Dead mothers
<i>vab-19</i> / T22D2.1	Ankyrin / Kank	WT	5% Emb; 5% Bmd
<i>pfd-2</i> / H20J04.5	Prefoldin / PFDN2	5% Emb	5% Emb + 50% Bmd
<i>klp-3</i> / T09A5.2	Motor kinesin Kar3/Ncd	WT	10% Emb + 10% Bmd
<i>farl-11</i> / F10E7.8	FAM40A/FAM40B	WT	30-40% Bmd
<i>cct-1</i> / T05C12.7	Chaperonin / TCP1	50% Emb; low progeny	70% Bmd
<i>cct-4</i> / K01C8.10	T complex chaperonin/ CCT4	30-40% Emb	10% Emb + 30% Bmd
<i>zyg-9</i> / F22B5.7	XMAP215/Dis1 family MAP	95% Emb	90%Emb +5-10% Bmd
<i>cct-2</i> / T21B10.7	T complex chaperonin/ CCT2	30% Emb	20% Emb + 30% Bmd
<i>ebp-2</i> / VW02B12L.3	EB-type microtubule binding	WT	5% Bmd
<i>klp-17</i> / W02B12.7	Motor kinesin Kar3/Ncd	WT	20% Emb
W07G1.1	Doublecortin domain-containing 2 / DCDC 2	WT	WT
W07G1.5	DCDC 2	WT	WT
<i>tac-1</i> / Y54E2A.3	TACC1	50-60% Emb	50% Emb+ 10% Bmd
<i>cct-3</i> / T21B10.7	T complex chaperonin/ CCT3	30% Emb; low progeny	50% Bmd
F54A3.2	XMAP215/Dis1 family MAP	WT	10% Emb
<i>klp-1</i> / unc-104 / C52E12.2	Kinesin-like motor / ATSV	WT	10% Emb
<i>ect-2</i> / T19E10.1	RhoGEF / Pebble	80% Emb	80% Emb
<i>let-805</i> / H19M22.2 *	myotactin	100% Bmd	95% Bmd
<i>cct-5</i> / C07G2.3	T complex chaperonin/ CCT5	30% Emb	30% Bmd
<i>klp-6</i> / R144.1	Monomeric kinesin KIF14	WT	40% Bmd
<i>cct-6</i> / F01F1.8	T complex chaperonin / CCT6A	20-30% Emb	50-60% Bmd
<i>pfd-5</i> / R151.9	Prefoldin / PFDN5	20% Emb	10% Emb + 40% Bmd
<i>dlc-1</i> / T26A5.9	Dynein light chain/ DYNLL1&2	WT	20%Emb + 10% Bmd

cls-1 / C07H6.3	CLASP	WT	10% Emb
cls-2 / R107.6	CLASP	10% Emb	20% Bmd
cls-3 / C07H6.3	CLASP	WT	10% Emb
unc-116/ khc-1/ R05D3.7	Kinesin heavy chain	10% Emb	10% Emb
aak-1/ PAR2.3	Catalytic subunit AMPK	WT	20% Emb
klp-7/ K11D9.1	XKCM1/MCAK kinesin	30-40% Emb	40% Emb + 20% Bmd
dhc-4/ W05B2.4	Dynein heavy chain	WT	5-10% Bmd
sup-35/ Y48A6C.3	RMND1 (Human regulator of microtubule dynamics 1)	WT	20% Emb + 20% Bmd
arf-6/ Y116A8C.12	ARF6 GTPase	WT	WT
klp-19/ Y43F4B.6	plus-end MT motor Kinesin-4	10% Emb	20-30% Bmd
lis-1/ T03F6.5	LIS1 (MAP)	20% Emb	50% Emb + 20% Bmd
zyg-8/ Y79H2A.11	DCX doublecortin	WT	WT
let-502*/ C10H11.9	ROCK Rho kinase	80% Bmd	100% Bmd
pig-1/ W03G1.6	MELK	WT	20% Bmd
bicd-1/ C43G2.2	Bicaudal-C	WT	WT
egal-1/ C10G6.1	EXD1	WT	10% Bmd
unc-44/ B0350.2	Ankyrin	10% Emb	60% Bmd
dyci-1/C17H12.1	Dynein intermediate chain	80-90% Emb	80-90% Emb
klp-10/C33H5.4	KIF15 kinesin-like	30% Emb	40% Emb + 30% Bmd
klp-18/C06G3.2	KIF15 kinesin-like	WT	20% Bmd
tbce-1/ K07H8.1	TBCEL tubulin cofactor E	WT	30% Bmd
klp-11/F20C5.2	Kinesin II	WT	10% Bmd
dnc-1/ZK593.5	P150 dynactin	80-90% Emb	90% Emb
klc-1/M7.2	Kinesin light chain	WT	WT
pfd-1/C08F8.1	Prefoldin / PFDN1	30% Emb	30% Emb + 30% Bmd
pfd-4/B0035.4	Prefoldin / PFDN4	WT	30% Emb + 20% Bmd
klp-12/T01G1.1	KIF21B Kinesin	WT	10% Bmd
dlc-2 / M18.2	Dynein light chain/ DYNLL1&2	Ste	Ste
dli-1/C39E9.14	Dynein light intermediate chain	70% Emb	60% Emb + 10% Bmd
eps-8/ Y57G11C.24	EPS8	WT	30% Bmd
cct-8/ Y55F3AR.3	Chaperonin CCT8	WT	30% Bmd
cct-7/ T10B5.5	Chaperonin CCT7	50% Emb	50% Bmd + 40% Bmd
spas-1/C24B5.2	spastin	WT	20% Bmd
noca-1/ T09E8.1	ninein	WT	40% Bmd
par-1/H39E23.1	MARK1/ Par 1	50% Emb	60-70% Emb
R10D12.10	Tau-tubulin kinase 1	WT	30% Bmd
F14H3.12	MARK1/ Par-1	WT	20% Bmd
ebp-1/Y59A8B.7	EB1	WT	30% Bmd
eel-1/Y67D8C.5 *	Hect domain E3 ligase	WT	20% Bmd
klp-2/osm-3/M02B7.3	Kinesin-like KIF17	WT	20% Bmd
klp-5/vab-8/K12F2.2	Kinesin-like KIF26B	WT	10-20% Bmd
kin-29/ F58H12.1	Serine threonine kinase SIK3	WT	30-40% Bmd
coel-1/C52B9.3	Tubulin-specific cofactor E	WT	WT
klp-8/C15C7.2	Kinesin-like	WT	10-20% Bmd
klp-4/F56E3.3	Kinesin-like KIF13A	20% Emb + 20% Bmd	10-20% Bmd
klp-13/F22F4.3	Kinesin-like KIF19	WT	10% Bmd
sad-1/ F58H12.1	serine threonine kinase BRSK2	WT	10% Bmd
aak-2/ T01C8.1	Catalytic subunit AMPK	WT	10% Bmd
C27C12.1	CLASP2	WT	WT
pqn-34/ptrn-1/F35B3.5	patronin	WT	10% Bmd
T08D2.8	Mini spindles	WT	10-20% Bmd WT
ani-1/Y49E10.19	Anillin	10% Emb	did not grow
cogc-1/mig-30/ Y54E10A.2	Golgi complex subunit 1	WT	WT
cogc-3/mig-29/	Golgi complex subunit 3	WT	WT

Y71F9AM.4			
<i>rabx-5/ Y39A1A.5</i>	Rab5 GEF	WT	10% Bmd
<i>csn-5/ B0547.1</i>	COP9 signalosome CSN5	WT	20% Bmd
<i>lam-1*/ W03F8.5</i>	laminin beta	100% Emb + low prog.	50% Emb + 50% Bmd
<i>cogc-2/ C06G3.10</i>	Golgi complex subunit 2	WT	WT
<i>ima-3/ F32E10.4</i>	importin alpha	20% Emb	40% Bmd
<i>zen-4/ klp-9/ M03D4.1</i>	Kinesin-like KIF23	100% Emb	100% Emb
<i>prkl-1/ ZK381.5</i>	Prickle	WT	WT
<i>arf-3/ F57H12.1</i>	ARF5	sterile mothers	sterile mothers
<i>vha-17/ F49C12.13</i>	V-ATPase subunit	WT	WT
<i>col-2/ W01B6.7</i>	collagen	WT	WT
<i>his-48/ B0035.8</i>	H2B histone	100% Emb	60% Emb + 20% Bmd
<i>par-5/ ftt-1/ M117.2</i>	14-3-3 protein	60% Emb	60% Emb
<i>sec-24.2/ ZC518.2</i>	SEC24B	30% Emb	40% Emb
<i>gex-3/ F28D1.10</i>	NCKAP1/ Kette	WT	30-40% Bmd
<i>mbk-2/ F49E11.1</i>	Minibrain/ DYRK2 kinase	WT	30% Bmd
<i>let-99/ K08E7.3</i>	DEP domain	70% Emb + 10% Bmd	30% Emb + 10% Bmd
<i>sas-6/ Y45F10D.9</i>	Hs-SAS-6	60% Emb	50% Emb
<i>csn-4/ Y55F3AM.15</i>	COP9 signalosome CSN4	WT	WT
<i>vps-18/ W06B4.3</i>	VPS18	WT	WT
<i>ral-1/ Y53G8AR.3</i>	Ras-related Ral-A	did not grow	did not grow
<i>rab-1/ C39F7.4</i>	Ras-related Rab-1A	sterile mothers	sterile mothers
<i>gad-1/ T05H4.14</i>	WD-repeat protein 70	WT	WT
<i>aps-1/ F29G9.3</i>	AP-1 sigma 2 subunit	low progeny, sick mother	90% late Emb, low progeny
<i>vps-37/ CD4.4</i>	Vps-37B ESCRT-I complex	WT	20% Bmd
<i>rga-3/ K09H11.3</i>	Rho GAP	20-30% Emb	20% Bmd
<i>air-1/ K07C11.2</i>	Aurora-A kinase	90% Emb	60% Emb
C13F10.2	KXD1 domain (cargo sorting)	WT	WT
<i>rbx-1/ZK287.5</i>	E3 ligase RBX1	90% Emb	90% Emb
<i>sas-5/ F35B12.5</i>	coiled coil (centriole assembly)	90% Emb	60% Emb+ 10% Bmd
<i>sun-1/ F57B1.2</i>	SUN domain	40% Emb + 10% Bmd	40% Emb + 10% Bmd
<i>atn-1/ W04D2.1</i>	alpha-actinin	WT	WT
<i>vps-54/ T21C9.2</i>	Vps54p GARP complex	WT	10% Bmd
<i>vps-33.1/ B0303.9</i>	VPS33A	WT	WT
<i>vps-33.2/ C56C10.1</i>	VPS33A	WT	WT
<i>vps-11/ R06F6.2</i>	VPS11	50% Emb + 10% Bmd	50% Emb + 10-20% Bmd
<i>vps-52/ F08C6.3</i>	Vps52p GARP complex	WT	20-30% Emb
<i>sec-10/ C33H5.9</i>	EXOC5 exocyst complex	40% Emb	20% Emb
<i>lam-2*/ C54D1.5</i>	laminin gamma	sterile mothers	90%-100% Bmd
<i>sec-15/ C28G1.3</i>	EXOC6 exocyst complex	WT	WT
<i>sdpn-1/ F45E1.7</i>	syndapin	WT	WT
<i>rab-8/ D1037.4</i>	Rab-8b GTPase	WT	WT
<i>rab-6.1/ F59B2.7</i>	Rab-6 GTPase	WT	WT
<i>rab-7/ W03C9.3</i>	Rab7 GTPase	60% Emb	50% Emb + 20% Bmd
<i>rab-10/ T23H2.5</i>	Ras-related Rab10	WT	WT
<i>sep-1/ Y47G6A.12</i>	separase	90% Emb	50% Emb+ 10% Bmd
<i>unc-37/ W02D3.9</i>	tran-1sducin-like Groucho	70% Bmd + 30% Emb	80% Bmd + 20% Emb
<i>csc-1/ Y48E1B.12</i>	aurora B complex member	WT	WT
<i>mlc-4/ C56G7.1 *</i>	myosin light chain	sterile mothers	sterile mothers
<i>pak-1/C09B8.7 *</i>	PAK1	WT	90%-100% Bmd
<i>dnc-2/ C28H8.12</i>	p50/ dynamitin/ DCTN2	30% Emb	30% Emb + 20% Bmd
<i>dnc-4/ C26B2.1</i>	p62/ dynactin/ DNTN2	WT	WT
<i>rab-27/ aex-6/ Y87G2A.4</i>	RAB27B	WT	WT
<i>csn-2/ B0025.2</i>	COP9 signalosome COPS2	WT	40% Bmd
<i>sur-6/ F26E4.1</i>	PP2A regulatory B subunit	20% Emb	20% Emb + 70% Bmd
<i>cul-2/ ZK520.4</i>	cullin-2	100% Emb	80% Emb
<i>vps-28/ Y87G2A.10</i>	VPS28	WT	30% Emb + 30% Bmd
<i>spn-4/ ZC404.8</i>	RNA-binding protein	did not grow	did not grow

<i>arf-1</i>/ B0336.2	ARF1 GTPase	10% late Emb	50% late Emb
<i>arx-1</i>/ Y71F9AL.16	ARP3	20-30% Emb	30% Emb + 30% Bmd
<i>csn-6</i>/ Y67H2A.6	COP9 signalosome COPS6	WT	20% Bmd
<i>rab-35/rme-5</i>/ Y47D3A.25	Rab35 GTPase	WT	WT
<i>syx-5</i>/ <i>syn-3</i>/ F55A11.2	syntaxin 5	molting problems, 10% Emb	70% Bmd
<i>sec-8</i>/ Y106G6H.7	exocyst complex SEC8	WT	10% Bmd
<i>vps-4</i>/ Y34D9A.10	VPS4B	WT	WT
<i>tpxl-1</i>/ Y39G10AR.12	TPX2	60% Emb	30% Emb + 20% Bmd
<i>vha-5</i>/ F35H10.4	V0 subunit ATPase	WT	WT
<i>rab-2</i>/ unc-108/ F53F10.4	Rab2A	WT	WT
<i>rab-8</i>/ D1037.4	Rab8B	WT	WT
<i>rab-39</i>/ D2013.1	Rab39B	WT	WT
<i>lgg-1</i>/ C32D5.9	GABARAP	WT	20% Bmd
<i>spdl-1</i>/ C06A8.5	spindle pole body component	WT	5% Bmd
<i>vps-32.1</i>/ C56C10.3	CHMP4A	40% Emb	30% Emb + 10-20% Bmd
<i>lin-5</i>/ T09A5.10	novel protein	40% Emb	50% Emb + 10+ Bmd
<i>air-2</i>/ B0207.4	Aurora kinase A	90% Emb + 10% Bmd	60% Bmd + 20% Bmd
<i>rab-21</i>/ T01B7.3	Rab21	WT	WT
<i>vps-51</i>/ B0414.8	Vps51p GARP complex	WT	WT
<i>rab-11.1</i>/ F53G12.1	Rab-11A	95% Emb	sterile mothers
<i>rab-8</i>/ D1037.4	Rab-8B	WT	WT
<i>noah-1</i>/ C34G6.6	NompA	sterile mothers	sterile mothers
<i>spd-5</i>/ F56A3.4	EEA1	100% Emb	80% Emb
<i>kca-1</i>/ C10H11.10	kinesin cargo adapter	50% Emb	30% Emb
<i>cye-1</i>/ evl-10/ C37A2.4	cyclin E	60% Emb + 20% Bmd	50% Emb + 50% Bmd
<i>efa-6</i>/ Y55D9A.1	Arf GEF	WT	WT
<i>evl-20</i>/ arl-2/ F22B5.1	ARL2	80% Emb	40% Emb + 40% Bmd
<i>rab-10</i>/ T23H2.5	Rab-10	WT	20% Emb
<i>bub-1</i>/ R06C7.8	BUB1	50% Emb	30% Emb
<i>inx-14</i>/ F07A5.1	innexin	40% Emb	40% Emb
<i>ran-4</i>/ R05D11.3	NTF2	60% Emb	60% Emb
<i>rba-1</i>/ K07A1.11	RBP4	95% Emb	40% Emb + 40% Bmd
<i>mel-26</i>/ ZK858.4	MATH & BTB/POZ domain	100% Emb	90% Emb
<i>rab-5</i>/ F26H9.6	Rab5	60% Emb	60% Emb
<i>spd-2</i>/ F32H2.3	coiled coil	WT	WT
<i>apr-1</i>/ K04G2.8	APC	WT	WT
<i>tlf-1</i>/ F39H11.2	TBP-like Factor 1	60% Emb	50% Emb + 50% Bmd
<i>tbcd-1</i>/ F16D3.4	beta-tubulin cofactor D	50% Emb	30% Emb
<i>sys-1</i>/ T23D8.9	novel protein	60% Emb + 20% Bmd	40% Emb + 30% Bmd
<i>cdc-26</i>/ B0511.9	APC/C component	40% Emb	40% Emb + 30% Bmd
<i>car-1</i>/ Y18D10A.17	LSM14	95% Emb	70% Emb
<i>tba-2</i>/ C47B2.3	alpha-tubulin	100% Emb	100% Emb
<i>agef-1</i>/ Y6B3A.1	ARFGEF1	40% Emb	40% Emb + 20% Bmd
<i>par-6</i>/ T26E3.3	Par-6	60% Emb	60% Emb
<i>apg-1</i>/ Y105E8A.9	AP-1 γ subunit	20% Emb + low progeny	40% Emb
<i>vps-4</i>/ Y34D9A.10	VPS4	did not grow	did not grow
<i>zyg-11</i>/ C08B11.1	ZYG11	30% Emb	20% Emb
<i>dyrb-11</i>/ T24H10.6	dynein light chain Roadblock 1	WT	WT
<i>ran-3</i>/ C26D10.1	RCC1	80% Emb	40% Emb + 30% Bmd
<i>mel-11</i>/ C06C3.1	myosin phosphatase	70% Emb	60% Emb
<i>tba-4</i>/ F44F4.11	alpha-tubulin	20% Emb	30% Emb + 10% Bmd
<i>Y19D2B.1</i>	alpha-tubulin	WT	WT
<i>die-1</i>/ C18D1.1	C2-H2 zinc finger	80% Emb + 20% Bmd	30% Emb + 70% Bmd
<i>ooc-3</i>/ B0334.11	nematode-specific RasGAP	30% Emb	20% Emb
<i>arp-1</i>/ Y53F4B.22	centractin	30% Emb	20% Emb + 40% Bmd
<i>gip-1</i>/ CeGRIP/H04J21.3	γ -tubulin ring complex	10% Emb	40% Emb

<i>ben-1/tbb-5/C54C6.2</i>	beta tubulin	10% Emb	30% Emb
<i>par-2/F58B6.3</i>	RING finger PAR2	80% Emb	50% Emb + 20% Bmd
<i>paa-1/F48E8.5</i>	PP2A structural subunit	90% Emb	10% Emb + 40% Bmd
<i>dcn-1/H38K22.2</i>	DCN-1-like protein 1	70% Emb	60% Emb
<i>par-3/F54E7.3</i>	Par3/Bazooka	30% Emb	30% Emb + 30% Bmd
<i>rabn-5/F01F1.4</i>	Rabaptin 5	WT	20% Bmd
<i>exos-9/F37C12.13</i>	EXOSC9/RRP45	WT	40% Bmd
<i>vps-2/Y46G5A.12</i>	CHMP2A	WT	30-40% Bmd
<i>apc-2/K06H7.6</i>	APC 2	50% Emb	20% Emb + 20% Bmd
<i>nmy-2/F20G4.3 *</i>	non-muscle myosin II	40% Emb + 10% Bmd	40% Emb + 50% Bmd
<i>vps-16/C05D11.2</i>	VPS16	30% Emb	30% Emb
<i>kap-1/F08F8.3</i>	kinesin-associated protein	WT	WT
<i>cyk-1/F11H8.4</i>	diaphanous/DIAPH1	WT	WT
<i>sas-4/F10E9.8</i>	CPAP	50% Emb	30% Emb + 20% Bmd
<i>ran-1/K01G5.4</i>	Ran GTP	dead mothers	dead mothers
<i>tbb-1/K01G5.7</i>	beta-tubulin	100% Emb	80% Emb + 10% Bmd
<i>gpr-2/C38C10.4</i>	GPR	WT	WT
<i>vha-14/F55H2.2</i>	D subunit of V-ATPase	WT	WT
<i>chc-1/T20G5.1</i>	clathrin heavy chain	100% Emb	70% Emb
<i>pod-1/Y76A2B.1</i>	coronin-7	40% Emb	50% Emb
<i>unc-32/ZK637.8</i>	subunit of V-ATPase	80% Emb	60% Emb + 40% Bmd
<i>rmd-1/T05G5.7</i>	RMDN1	WT	WT
<i>tsg-101/C09G12.9</i>	Vps23P/TSG101	WT	WT
<i>mup-4*/ZK1151.1</i>	novel transmembrane	40% L1 larval lethal	80% L1 larval lethal
<i>gei-4/W07B3.2</i>	waek homol. to trichohyalin	50% Emb	80% Emb + 10% Bmd
<i>ptc-1/ZK675.1</i>	Patched	WT	WT
<i>rga-2/Y53C10A.4</i>	RhoGAP	40% Emb	20% Emb
<i>lam-2/C54D1.5</i>	laminin gamma subunit	sterile mothers, few Bmd	90% Bmd
<i>ifb-1/F10C1.2</i>	intermediate filament B	WT	WT
<i>rpl-21*/C14B9.7</i>	ribosomal protein L21	low progeny + Emb	low progeny + Emb
<i>rnr-2*/C03C10.3</i>	ribonucleotide reductase	80% Emb	70% Emb
<i>lst-3*/Y37A1B.1</i>	CCAR1	dead mothers	dead mothers

Table S2. Strains used in this study

Strain	Genotype
N2	Wild-type
EG6699	<i>ttTi5605 II; unc-119(ed3) III; oxEx1578</i>
OD761	7 times outcrossed <i>let-502(sb118ts)</i>
ML752	4 times outcrossed <i>mcls35 [lin-26p::GFP::TBA-2; pat-4::CFP, rol-6(su1006)]</i>
ML1652	4 times outcrossed <i>mcls46 [pCL08 dlg-1p::DLG-1::RFP, Cb-unc-119(+)]</i> described in (Diogon et al., 2007)
ML1720	<i>mcls35; mcls46</i>
ML1649	<i>mcSi53[pML457 dpy-7p::EBP-2::GFP, Cb-unc-119(+)] II</i>
ML1654	<i>mcSi53; mcls46</i>
ML1658	<i>let-502(sb118ts); mcSi53; mcls46</i>
ML1840	<i>let-502(sb118ts); mcls46</i>
OD523	3 times outcrossed <i>ltSi63 [pOD1111 CEOP3608 TBG-1::GFP, Cb-unc-119(+)] II</i>
OD2509	<i>gip-2(lt19[gip-2::GFP]::loxP::Cb unc-119(+)::loxP) I; unc-119(ed3) III</i>
OD952	<i>ltSi246[pOD1270; noca-1p::noca-1abcfgh-superfolderGFP; Cb-unc-119(+)]II; unc-119(ed3)III</i>
ML2282	<i>mcls54 [pML497 dpy-7p::SPAS-1_IRES_NLSmCherry, Cb-unc-119(+)] X</i>
ML1968	<i>ltSi246; mcls54 X</i>
ML2552	<i>ltSi63; mcls54 X</i>
ML2554	<i>gip-2(lt19) I; mcls54 X</i>
ML1896	<i>mcls35; mcls54</i>
ML1931	<i>let-502(sb118ts); mcls54</i>
ML1765	<i>mcls35; mcEx574 [pML477 elt-3p::SPAS-1_IRES_mCherry; myo-2p::GFP]</i>
ML1772	<i>let-502(sb118ts) I; mcls35; mcEx574</i>
ML1766	<i>mcls35; mcEx575 [pML479 lin-26p::SPAS-1_IRES_mCherry; myo-2p::GFP]</i>
ML1771	<i>let-502(sb118ts) I; mcls35; mcEx575</i>
ML1768	<i>mcls35; mcls46; mcEx576 [pML485 ceh-16p::SPAS-1_IRES_mCherry; myo-2p::GFP]</i>
ML1769	<i>mcls35; mcls46; mcEx602 [pML485 ceh-16p::SPAS-1_IRES_mCherry; myo-2p::GFP]</i>
ML1770	<i>mcls35; mcls46; mcEx603 [pML485 ceh-16p::SPAS-1_IRES_mCherry; myo-2p::GFP]</i>
ML1802	<i>let-502(sb118ts) I; mcls35; mcls46; mcEx603</i>
ML1804	<i>let-502(sb118ts) I; mcls35; mcls46; mcEx576</i>
ML1805	<i>let-502(sb118ts) I; mcls35; mcls46; mcEx602</i>
ML1886	<i>mcls35; mcEx634 [pML472 hsp::SPAS-1_IRES_mCherry; myo-2p::GFP]</i>
ML1824	<i>mcls35; mcEx606 [pML494 dpy-7p::SPAS-1Δ_IRES_NLSmCherry; myo-2p::GFP]</i>
OD723	6 times outcrossed <i>noca-1(ok3692)V/nT1[qls51] (IV;V)</i>
OD726	6 times outcrossed <i>ltSi77[pOD1112; lbp-1p::mCherry; Cb-unc-119(+)]V</i>
OD739	<i>ltSi173[pOD1114; noca-1p::noca-1gh; Cb-unc-119(+)] II; unc-119(ed3)III; noca-1(ok3692)V</i>
OD758	<i>ltSi182[pOD1237; noca-1p::noca-1abcfgh; Cb-unc-119(+)]II; unc-119(ed3) III; noca-1(ok3692) V</i>
OD844	<i>let-502(sb118ts)I; ltSi77[pOD1112; lbp-1p::mCherry; Cb-unc-119(+)]V</i>

OD846	<i>let-502(sb118ts)I; noca-1(ok3692)V/nT1[qIs51](IV;V)</i>
OD907	<i>ltSi222[pOD1250/pSW078; Plbp-1::GFP-tbb-2-operon-linker-mCherry-his-11; cb-unc-119(+)]II; noca-1(ok3692)V/nT1[qIs51](IV;V)</i>
OD909	<i>ltSi222[pOD1250/pSW078; Plbp-1::GFP-tbb-2-operon-linker-mCherry-his-11; cb-unc-119(+)]II; ltSi77[pOD1112/pSW032; Plbp-1::mCherry; cb-unc-119(+)]V</i>
OD998	<i>ltSi246[pOD1270; noca-1p::noca-1abcfgh-superfolderGFP; Cb-unc-119(+)]II; noca-1(ok3692)V</i>
OD1252	<i>let-502(sb118ts)I; ItSi173[pOD1114; noca-1p::noca-1gh; Cb-unc-119(+)]II; noca-1(ok3692)V</i>
OD1253	<i>let-502(sb118ts)I; ItSi182[pOD1237; noca-1p::noca-1abcfgh; Cb-unc-119(+)]II; noca-1(ok3692)V</i>
OD1580	<i>ltSi518[pOD1338; noca-1p::noca-1acfgh(STOP codon in the first exon of isoform b); Cb-unc-119(+)]II; unc-119(ed3)III; noca-1(ok3692)V</i>
OD2422	<i>let-502(sb118ts)I; ltSi518[pOD1338; noca-1p::noca-1acfgh(STOP codon in the first exon of isoform b); Cb unc-119(+)]II; unc-119(ed3)III; noca-1(ok3692)V</i>
ML1617	<i>4 times outcrossed xnIs97 [pJN455(hmr-1p::HMR-1::GFP); Cb unc-119(+)] III, gift from J. Nance lab (Achilleos et al., 2010)</i>
ML1899	<i>xnIs97 III ; mcIs54/+ X</i>
ML1913	<i>let-502(sb118ts) I; xnIs97 III</i>
ML1915	<i>let-502(sb118ts) I; xnIs97 III; mcIs54/+ X</i>
ML2100	<i>let-502(sb118ts) I; xnIs97 III; rde-1(ne219) V; ksIs9 [lin-26p::RDE-1, rol-6(su1006), lin-26p::NLS-GFP]</i>
ML1861	<i>let-502(sb118ts) I; mcIs54/+ X; mcEx553 [pML1533 ceh-16p::GFP::MLC-4DD; myo-2p::GFP]</i>
ML1862	<i>let-502(sb118ts) I; mcIs54/+ X; mcEx555 [pML1523 mlc-4p::GFP::MLC-4DD; myo-2p::GFP]</i>
ML1867	<i>let-502(sb118ts) I; mcIs54 X; mcEx554 [pML1539 elt-3p::GFP::MLC-4DD; myo-2p::GFP]</i>
ML1312	<i>mcIs49[mlc-4p::GFP::MLC-4, pie-1p::GFP::MLC-4, pRF4]</i>
ML2493	<i>mcIs49; mcIs54 X</i>
ML2376	<i>syx-5(mc51)/oxTi711 [eft-3p::Td-tomato:::H2B, Cb unc-119(+)] V</i>
ML2379	<i>let-502(sb118ts) I; syx-5(mc51)/oxTi711 V</i>
ML2424	<i>xnIs97 III ; syx-5(mc51)/oxTi711 V</i>
ML2423	<i>let-502(sb118ts) I; xnIs97 III; syx-5(mc51)/oxTi711 V</i>
ML2490	<i>syx-5(mc51)/oxTi711 V ; mcIs54 X</i>
ML2324	<i>N2; mcEx871 [dpy-7p::GFP::SYX-5; myo-2p::mCherry]</i>